Cerebral Cortex, 2019;00: 1–12

doi: 10.1093/cercor/bhz095
Advance Access Publication Date: 4 June 2019
Original Article

ORIGINAL ARTICLE

Brain–Heart Interactions Underlying Traditional Tibetan Buddhist Meditation

Haiteng Jiang[1,7,#], Bin He[1,2,7,#,*], Xiaoli Guo[3], Xu Wang[3], Menglin Guo[3], Zhuo Wang[3], Ting Xue[4,5], Han Li[4,5], Tianjiao Xu[4], Shuai Ye[1,7], Daniel Suma[1], Shanbao Tong[3,*] and Donghong Cui[4,5,6,*]

[1]Department of Biomedical Engineering, Carnegie Mellon University, Pittsburgh, PA 15213, USA, [2]Center for Neural Basis of Cognition, Carnegie Mellon University, Pittsburgh, PA 15213, USA, [3]School of Biomedical Engineering, Shanghai Jiao Tong University, Shanghai, 200240, China, [4]Shanghai Mental Health Center, Shanghai Jiao Tong University School of Medicine, Shanghai, 200030, China, [5]Shanghai Key Laboratory of Psychotic Disorders, Shanghai Jiao Tong University, Shanghai, 200030, China, [6]Brain Science and Technology Research Center, Shanghai Jiao Tong University, Shanghai, 200240, China and [7]Department of Biomedical Engineering, University of Minnesota, Minneapolis, MN 55455, USA

Address correspondence to email: bhe1@andrew.cmu.edu, stong@sjtu.edu.cn, or manyucc@126.com. http://orcid.org/0000-0003-2944-8602

[#]Those authors contributed equally to the work

Abstract

Despite accumulating evidence suggesting improvement in one's well-being as a result of meditation, little is known about if or how the brain and the periphery interact to produce these behavioral and mental changes. We hypothesize that meditation reflects changes in the neural representations of visceral activity, such as cardiac behavior, and investigated the integration of neural and visceral systems and the spontaneous whole brain spatiotemporal dynamics underlying traditional Tibetan Buddhist meditation. In a large cohort of long-term Tibetan Buddhist monk meditation practitioners, we found distinct transient modulations of the neural response to heartbeats in the default mode network (DMN), along with large-scale network reconfigurations in the gamma and theta bands of electroencephalography (EEG) activity induced by meditation. Additionally, temporal-frontal network connectivity in the EEG theta band was negatively correlated with the duration of meditation experience, and gamma oscillations were uniquely, directionally coupled to theta oscillations during meditation. Overall, these data suggest that the neural representation of cardiac activity in the DMN and large-scale spatiotemporal network integrations underlie the fundamental neural mechanism of meditation and further imply that meditation may utilize cortical plasticity, inducing both immediate and long-lasting changes in the intrinsic organization and activity of brain networks.

Key words: meditation, consciousness, neurovisceral integration, EEG, ECG, default mode network

Introduction

Meditation, stemming from ancient Indian Ayurvedic medicine, is a mind and body self-regulatory practice that aims to cultivate well-being and insight into the true nature of all phenomena (Ekman et al. 2005). While its roots may be ancient and spiritual in nature, numerous recent scientific studies have demonstrated quantifiably beneficial effects in the psychological, neurological, and cardiovascular domains (Rubia 2009; Levine et al. 2017). A significant portion of research suggests that meditation is associated with improvements in attention control, emotion regulation, and self-awareness processing (Holzel et al. 2011; Tang et al. 2015) and that its practice results in large-scale spatiotemporal brain network reconfigurations, especially in the default mode network (DMN) (Brewer et al. 2011) and theta and alpha bands (7), as well as potential physiological changes in skin conductance and heart rate (Wallace 1970; Tang et al. 2009). Additionally, recent evidence supports a theory that correlations between heart rate fluctuation and DMN activity underlie meditation (Wong et al. 2007; Lutz et al. 2009; Ziegler et al. 2009).

Different cognitive processing modules work in parallel during meditation and could be mediated by rhythmic activities at different time scales (Buzsaki and Draguhn 2004). Low frequency oscillations (<30 Hz) reflect top-down information processing involving attention and working memory retention, whereas high frequency oscillations (>30 Hz) reflect bottom-up processing of the contents of experience (Razumnikova 2007). Specific cognitive states such as attentiveness (e.g., focused vs. distracted) and wakefulness (e.g., alert vs. drowsy) have been associated with predictable oscillatory changes (Saggar et al. 2012). While individual oscillation can be linked to specific cognitive processes, different oscillations can work in concert (Canolty and Knight 2010). For example, stronger theta–gamma coupling has been shown to be related to attention modulations (Canolty et al. 2006; Voloh et al. 2015). Therefore, we believe that the patterns of neuronal oscillations may additionally be used to interpret and discern the numerous cognitive processes involved in meditation.

In the Tibetan Buddhist tradition, meditation is typically performed via two practices: samatha and vipassana. Samatha aims to calm the mind by maintaining focus on an object (such as an image of Buddha or a mantra) for an extended period of time. In combination with the focus and stability provided by practicing samatha, vipassana meditation enables one to enhance meta-awareness, cultivate an accurate understanding about one's identity and the nature of the world, and develop liberating wisdom (Wallace 2006). To gain true insight, samatha and vipassana need to be integrated. As is common with long-term practitioners of any skill, veteran meditators can more reproducibly generate stable mental states than their unexperienced counterparts (Lutz et al. 2007). By investigating the stable meditative practices of the highly experienced Tibetan Buddhist monks, we hope this work will shed new light on the neural mechanisms of meditation as well as its possible long-term effects on the brain and body.

Given the significant evidence that meditation is a bidirectional process involving both the mind and body, potentially involving communication between the central nervous system (CNS) and autonomic nervous system (Thayer and Lane 2000), it is essential for our understanding of its mechanism that we investigate the dynamics of these interactions on multiple spatial and temporal scales. Internal organs, such as the heart, act as spontaneously occurring stimuli, sending information to and being monitored by the CNS through homeostatic regulation (Park and Tallon-Baudry 2014). Noting that extensive research has demonstrated an association between the neural processing of cardiac afferent signals with visual awareness (Park et al. 2014), selfhood (Babo-Rebelo et al. 2016), and bodily self-consciousness (Park et al. 2016), others have previously proposed that these interactions guide subjective experiences and regulate the organism's homeostasis (Craig 2009). As current understanding defines meditation as a "unique state of consciousness"(Michaels et al. 1976), which has been previously linked to enhanced body awareness and reduced self-referential processing (Holzel *et al.* 2011), it is reasonable to hypothesize that meditation induces changes in both the neural response to cardiac activity and large-scale spatiotemporal brain networks. Specifically, we hypothesize that 1) As awareness of the heartbeat may be considered a distracter to the object of meditation, the neural response to cardiac signals is altered in conflict monitoring regions, such as anterior cingulate cortex (ACC) during meditation (van Veen et al. 2001). 2) As sustained attention is the central element of Tibetan Buddhist meditation training, we hypothesize that the behavioral elements associated with the long-term practice of meditation might induce changes in the brain networks dedicated to attention, which are proportional to an individual's meditative experience.

Here, we tested these hypotheses by investigating 60 long-term traditional Tibetan Buddhist monks with varying meditation experience (5–35 years) and 25 matched local meditation-naive controls through simultaneous electroencephalography (EEG)–electrocardiogram (ECG) recordings during resting and meditative states. Specifically, we investigate the involvement of the heartbeat-evoked potential (HEP) and its potential to reflect the effects of cardiac activity on neural activity through the study of average heartbeat time-locked EEG signals (Fig. 1) (Montoya et al. 1993). In addition, by utilizing advanced EEG source reconstruction techniques (Van Veen et al. 1997; Gross et al. 2001; He et al. 2011), spatiotemporal brain network reconfigurations were examined at the source level through within-frequency (Nolte et al. 2004) and cross-frequency (Jiang et al. 2015) whole brain network connectivity analyses.

Materials and Methods

Subjects

With the help of Kambo Suo Lang in the Qiongke Temple and Kambo Kharong in the Jiaqu Temple in Tibetan area, 60 Tibetan Buddhist male monks and 25 male volunteers from the same area were recruited (Qiongke Temple: 36 monks with Gelug tradition of Tibetan Buddhism, 12 local controls; JiaQu Temple: 24 monks with Nyingma tradition of Tibetan Buddhism, 13 local controls). All subjects were healthy without neurological/psychiatric disorders, brain injury, cardiovascular disease, or drug/alcohol addictions. The Tibetan Buddhist monks trained their minds through 2 meditation practices, samatha and vipassana, for at least 2 h a day for 5–35 years (18.15 ± 8.25 years). Samatha is the Buddhist practice of calm abiding, which steadies and concentrates the mind by resting the attention on a single object or mantra. Vipassana is a clear-seeing or insight meditation practice, which enables one to inquire into the true nature of all phenomena, resulting in wisdom. It is commonly believed that samatha practice establishes a mindfulness state as a prelude, which is then used for insight practice (vipassana) (Wallace 2006). By integrating both samatha and vipassana in sequence,

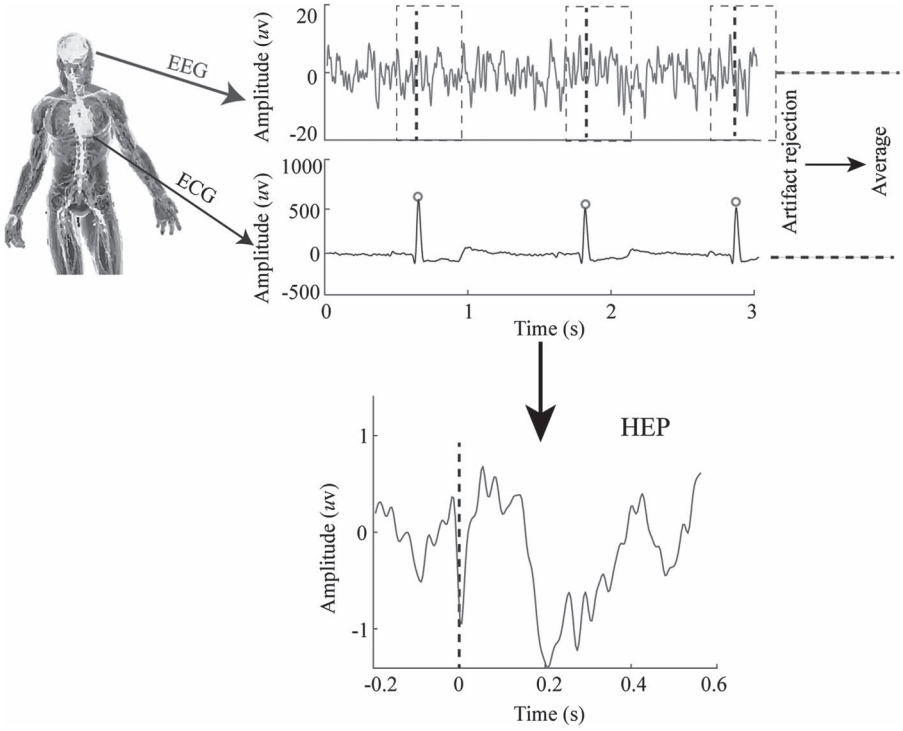

Figure 1. Schematic illustration of the HEP. Ongoing EEG brain acitvity is aligned to the ECG activity (R peak) indicated by the red circles. After artifact rejection, the HEP is obtained by averaging over all clean EEG signals time-locked to ECG R peaks.

it is believed that meditation can lead a practitioner to full enlightenment or liberation—the deepest form of well-being. Meditation-naive Tibetan controls from a nonmonastic environment were recruited from the local regions with matched race, age, sex, culture, and living background. Although the Tibetan controls also recite the mantra daily, as part of their religious beliefs, it should be pointed out that chanting the mantra does not represent meditation and that Tibetans who do not practice regular meditation could not attain a meditative state. Due to the extreme sparsity of those who qualified as control subjects in the region, it was difficult to recruit sufficient numbers, leading to unequal populations of monks and control subjects. Eight monks that occasionally opened their eyes during meditation were excluded from further analysis. There were no significant age differences between the monks (40.9 ± 8.3 years) and controls (40.2 ± 9.0 years) [$t(75) = 0.36$, $P > 0.70$] used in this work. The study was approved by the local Institutional Review Boards, and all subjects provided written consent in accordance with the Helsinki Declaration.

Task Protocol and EEG–ECG Recordings

Subjects were asked to be in a relaxed and nonmeditative resting state with eyes closed for 10 min. Following an auditory cue, the monk subjects were instructed to start meditating in a similar manner to their daily practice for 30 min. All monks meditated via a 7-point posture of Vairocana, in which the shape of the body was similar to the form of an Egyptian pyramid. This special posture is thought to be the best way to achieve tranquility and peace. To enter the meditation state, there are 3 meditation techniques: using an object, reciting a mantra, and "watching" the breath. When using an object, the practitioner is to rest the mind lightly on an object, such as an image of the Buddha or of a powerful master that invokes a special feeling of inspiration. Reciting a mantra unites the mind, which is used a great deal in Tibetan Buddhism, and can help achieve inner peace. "Watching" the breath is to rest one's attention, lightly and mindfully, on the breath. Each of these methods forms a complete meditation practice on its own, but can also be combined. In general, Tibetan Gelug and Nyingma monks do not use the breath as an object of meditation (Johnson 2004), but rather focus on different techniques to achieve a meditative state. Gelug monks prefer reciting a mantra to unite the mind while Nyingma monks tend to rest the mind lightly on an object, such as an image of the Buddha. The EEG and ECG signals were recorded continuously with a 64-channel Ag/AgCl EasyCap^{TM} (Brain Products GmbH). One channel was used for ECG recording by placing an electrode on the chest, while all others were used for scalp EEG recordings. All electrodes were referenced to FCz, and impedances were kept below 10 kΩ. The signals were amplified using the BrainAmp amplifier (Brain Products GmbH) and sampled at 1000 Hz. All monks reported that they achieved a mindfulness meditative state similar to their daily practice during the experiment. In this work, we focus on the deep meditative state, which was selected as the last 10 min of each monk's meditation.

EEG Data Analysis

EEG data were analyzed using Matlab R2016a (MathWorks, Inc.) and the Fieldtrip toolbox (Oostenveld et al. 2011). Raw EEG data from both rest and meditation conditions were epoched into 2 s segments with no overlap. In each epoch, a notch filter at 50 Hz was applied to remove power line

noise, and visual inspection was carefully conducted to reject segments containing nonphysiological artifacts. After that, subject- and task-specific independent component analysis (ICA) was performed to remove possible eye blink, movement, and heartbeat artifacts. The number of components (control rest: 8.02 ± 2.50; monk rest: 7.97 ± 2.52; monk meditation: 7.36 ± 2.26) and the percentages of explained variances removed (control rest: $14.87\% \pm 11.77\%$; monk rest: $17.58\% \pm 12.11\%$; monk meditation: $15.14\% \pm 11.12\%$) did not differ between conditions (all $P > 0.20$). These artifact-free data were then common average re-referenced.

HEP Analysis

The HEP was computed by averaging EEG signals around the ECG R peaks for each condition. ECG R peaks were detected by a "sym4" wavelet decomposition technique. In this technique, ECG time series were decomposed down to level 5 and reconstructed using only the wavelet coefficients from levels 3 to 5, which covered the maximized QRS passband. R peaks were then identified by finding the local maxima in the squared magnitude of the reconstructed time series and subsequent visual inspection. Then, EEG signals 200 ms before and 600 ms after the onset of each R peak were extracted. To further attenuate the cardiac field artifacts and other noncortical physiological activities, subject- and task-specific ICA was employed a second time. The number of removed components (control rest: 8.38 ± 0.92; monk rest: 7.95 ± 1.32; monk meditation: 7.97 ± 1.30) and the percentages of explained variances in the removed components (control rest: $14.29\% \pm 7.69\%$; monk rest: $14.59\% \pm 10.05\%$; monk meditation: $15.15\% \pm 10.79\%$) were not significantly different between conditions (all $P > 0.15$). After artifact correction, clean epochs were averaged to compute the HEP.

Surrogate R Peaks

To investigate whether the HEP modulation difference is time-locked to the original R peaks or just a product of the natural nonheart linked EEG dynamics, we created surrogate R peaks by randomly shifting all original R peak onsets by the same amount of time (−400 ms–400 ms). This technique was performed 200 times for each condition and subject, separately, with each shift being drawn from a normal distribution, generating unique synthetic data with identical temporal statistical properties to the original R peaks.

Source Localization Analysis

To localize the underlying source activity, we applied 2 types of beamforming approaches. Dynamic imaging of coherent sources (DICS) (Gross et al. 2001) was used to identify the spatial source distributions in the delta (1–4 Hz), theta (4–8 Hz), alpha (8–12 Hz), beta (12–30 Hz), and gamma (30–48 Hz) frequency bands. Given the likelihood that the higher frequencies still contained muscle artifacts, even after data cleaning (Muthukumaraswamy 2013), we limited our maximum gamma-band frequency to 48 Hz. The time series of sources were then reconstructed by a linearly constrained minimum variance (LCMV) beamformer (Van Veen et al. 1997) and were later used for HEP source localization and cross-frequency analysis. The leadfield, calculated using a Colin27 Montreal Neurological Institute (MNI) template and boundary element model in the FieldTrip toolbox, was 8 mm spaced with 3898 equally distributed grid points in the gray matter. Then, DICS spatial filters were constructed from the leadfield and a cross-spectral density matrix to maximize the activity of interest at each specific grid point, while suppressing the contribution of all other grid points. Spatial filters were also applied to Fourier-transformed sensor level data to estimate power and within-frequency connectivity at the source level. Here, we also used an LCMV beamformer to extract the time course of every epoch at each grid point with 5% regularization. In the HEP source localization, source activities were averaged over the time window where significant differences between conditions or groups at the sensor level were identified by the cluster permutation test detailed below.

Connectivity Analysis

To assess all-to-all connectivity maps at the source level, we segmented the whole brain into 90 region of interest (ROI) according to the Automated Anatomical Labeling template based on the Colin27 MNI model (Tzourio-Mazoyer et al. 2002). Apart from the cerebellum, all cortical and subcortical regions are included (Supplementary Table S1). To avoid bias due to size differences, as each ROI has a different number of grid points, we selected the centroid of each as the representative position, with the centroid being defined as the grid point with the minimum Euclidean distance to all other grid points inside the ROI. Thus, functional connectivity maps at each frequency band were based on $(90 \times 89/2 =)$ 4005 pairs of connections (90×90 2D matrix). As a measurement of within-frequency functional connectivity, we used the imaginary part of coherence, which is insensitive to the false connectivity that arises from volume conduction (Nolte et al. 2004). Since power differences could potentially bias the connectivity estimation, we applied stratification techniques to obtain a subset of matched epochs with identical power distributions between 2 contrasts, or as equivalent as possible, given the finite number of epochs. When comparing 2 conditions (e.g., monk meditation to monk rest), the maximal power epoch from the high-power condition and the minimal power epoch from the low-power condition were removed sequentially until means of the 2 remaining distributions were approximately the same. When comparing 2 groups (e.g., monk rest vs. control rest), we used a median split strategy in which we ensured no significant power differences between the 2 groups by including only the higher-part epochs from the low-power group and the lower-part epochs from the high-power group.

Apart from within-frequency functional connectivity, we also investigated directional interactions between different frequencies through cross-frequency directionality (CFD) (Jiang et al. 2015). CFD is a way to estimate whether the phase of a slow oscillation leads the amplitude of a fast oscillation or the converse. Essentially, CFD is based on the phase-slope index (PSI) between the phase of a slow oscillation and the power envelope of a fast oscillation and measures the information flow between the 2 signals (Nolte et al. 2008). A positive PSI indicates that the seed region is the sender while a negative value represents that it is the receiver. Similarly, a positive CFD value indicates that the phase of a slow oscillation drives the power envelope of a fast oscillation with the inverse occurring for negative values. To compute the CFD at the source level, we performed the analysis utilizing the phase of the frequencies from 2 to 22 Hz, at a step of 1 Hz, and the amplitude of the envelope of the frequencies from 30 to 120 Hz, in 5 Hz increments. Through this analysis, the whole brain CFD for each subject and each condition is

calculated as a 4D $21 \times 19 \times 90 \times 90$ matrix (phase frequency bins∗amplitude frequency bins∗ROIs∗ROIs).

Statistical Analysis

A nonparametric cluster permutation test was applied to compare differences between groups (monk rest vs. control rest) and conditions (monk meditation vs. monk rest) while controlling for multiple comparison (Maris and Oostenveld 2007). At the sensor level for the HEP statistic, an independent (or dependent) 2-sample *t*-test was performed between groups (or conditions) over individual samples in the time window from 0 to 600 ms after the ECG R peaks. All individual samples with *t* values exceeding the threshold ($P < 0.05$) became cluster candidates and were subsequently clustered based on their spatial-temporal adjacency. The cluster score was defined as the sum of the *t* values over the individual samples within the cluster and the reference distribution was obtained by selecting the maximum summed cluster *t*-statistic from randomly shuffled group or condition labels (1000 permutations). Significant clusters were obtained by comparing the observed cluster scores to the 95th percentile of the reference distribution (2-tailed, $P < 0.05$). For the source level statistic, the procedure was similar, except that each cluster was formed based on spatial adjacency instead of spatial-temporal adjacency. The HEP source statistic was applied to source activities averaged over the 280–320 ms (long-term meditation effect: monk rest vs. control rest) and 340–360 ms (immediate meditation effect: monk meditation vs. monk rest) time segments following the R peak.

Network-based statistics (NBS) were utilized to compare connectivity differences between groups (monk rest vs. control rest) or conditions (monk meditation vs. monk rest) (Zalesky et al. 2010). Each network connection was evaluated for statistical significance using an independent (or dependent) 2-sample *t*-test between groups (or conditions). Topological clusters were formed from the pruned graphs ($P < 0.005$) and were assigned a cluster score based on their internal degree. The cluster with the maximum number of connections was used as a test statistic. As before, by randomizing the data across groups or conditions and recalculating the test statistic 5000 times, we generated a reference distribution of maximum cluster connection values, which was used to evaluate the statistics of the observed topological clusters. When investigating the association between network connectivity and meditation experience, the procedure is similar. Here, the difference is that we used Pearson correlation as the statistical metric and shuffled meditation experiences across subjects during permutation. These statistics were performed with the open source NBS toolbox (http://www.nitrc.org/projects/nbs). Network visualization used circlize package in R (Gu et al. 2014) and BrainNet Viewer toolbox (Xia et al. 2013).

Results

Immediate Meditation Effects: Monk Meditation versus Monk Rest

To identify the immediate effects of meditation, we contrasted the meditation and rest states within monks. The HEP amplitude was found to be significantly different over the right central and frontal sensors between 340 ms and 360 ms post R peak (Fig. 2A,B; cluster *t*-statistic) with the mean being smaller during meditation than rest [Fig. 2C; paired *t*-test, $t(102) = 1.9$, $P < 0.05$]. Control analysis revealed that all cluster *t*-statistics resulting from surrogate R peaks (see Materials and Methods) were smaller than the true R peak (Monte Carlo 200 iterations, $P < 0.05$), confirming that the difference in HEP amplitude is temporally locked to the heartbeat. Next, in order to discern the underlying neural activity of the differential HEPs (monk meditation vs. monk rest) found at the sensor level in response to meditation, we performed source reconstruction, uncovering a significant cluster, which encompasses the bilateral ACC and extends to the superior medial frontal gyrus (peak MNI coordinate: [14 40 20]; cluster size: 179 vertices; Fig. 2D; cluster *t*-statistic). In the continuous, non-ECG R peak synced neural activity, increased posterior gamma power was found during meditation (Supplementary Fig. S1A). Moreover, NBS (Zalesky et al. 2010) revealed significantly decreased connectivity in the gamma band of the frontal-limbic network (Fig. 2G). This network was composed of 29 regions and 52 connections (Fig. 2E; Supplementary Table S2) and mainly consisted of the left inferior frontal gyrus (opercular part), right superior frontal gyrus (dorsolateral part), left caudate nucleus, and left insula (Fig. 2F). Notably, HEP modulation ($|\frac{meditation-rest}{rest}|$) was also found to be positively correlated with this modulation of gamma network connectivity (Fig. 2H; $r = 0.44$, $P < 0.001$).

Long-Term Meditation Effects: Monk Rest versus Control Rest

As with any other skillset, the long-term practice of meditation can induce plastic, potentially long-term changes in the brain (Davidson and Lutz 2008). To investigate the effects of long-term meditation, we compared the resting state of the Tibetan Buddhist monks with that of the controls. HEP amplitude was found to significantly differ over the frontal-central sensors between 280–320 ms after ECG R peaks (Fig. 3A,B; cluster *t*-statistic), with the monks displaying a smaller HEP (more positive) during their resting state [Fig. 3C; 2-sample *t*-test, $t(75) = 3.2$, $P < 0.005$]. Again, the control surrogate R peak analysis revealed that the observed difference in EEG signals is time-locked to heartbeat (Monte Carlo, $P < 0.01$). Source analysis revealed that the difference in HEPs (monk rest vs. control rest) was localized to 2 separate clusters containing multiple regions (Fig. 3D; cluster *t*-statistic): one extending across the posterior cingulate cortex (PCC) and precuneus bilaterally (peak MNI coordinate: [−1 −37 32]; cluster size: 147 vertices) and another in the right medial prefrontal cortex (mPFC) (peak MNI coordinate: [34 32 34]; cluster size: 81 vertices). We further observed that the Buddhist monks exhibited decreased frontal theta activity (Supplementary Fig. S1B) and reduced parietal-central and parietal-limbic network connectivity in the theta band (Fig. 3G,E; 40 regions, 53 connections; Supplementary Table S3) More specifically, these alterations were seen primarily within the bilateral precuneus, left supplementary motor area, and right superior parietal gyrus (Fig. 3F).

After noting that ongoing decreased theta connectivity is associated with monk meditators at rest, we investigated whether the brain network connectivity strength in the theta band varies in proportion to meditation experience. Given that age is significantly correlated with the length of meditation experience in the monks ($r = 0.71$, $P < 1 \times 10^{-8}$), we use age as the covariate factor in the network-based correlational statistical analysis. As shown in Figure 4A, this analysis revealed that theta band connectivity in a temporal-frontal network negatively correlated with meditation experience ($r = -0.69$, $P < 1 \times 10^{-9}$) (Fig. 4C). Said network predominantly consisted of the right

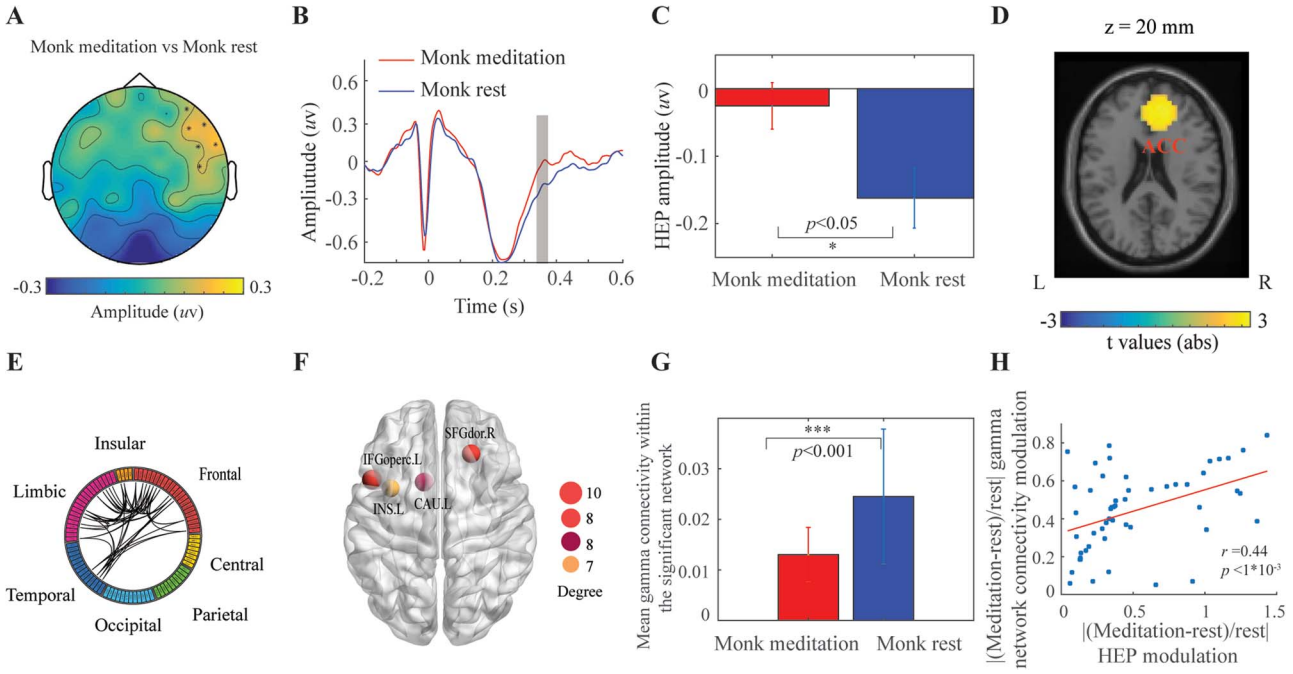

Figure 2. Immediate meditation effects determined by comparing monk meditation to monk rest. A–D: HEP effects. (*A*) HEP topological difference maps during which the significant difference is observed (340–360 ms post R peak). Dots mark the locations of sensors above the significant clusters. (*B*) Time course of HEP averaged across the marked sensors in A. The shaded area indicates the time period containing the significant differences identified by cluster statistics (cluster level, $P < 0.05$). (*C*) Mean HEP amplitude averaged across the marked sensors during the 340–360 ms following the R peak for monk meditation and monk rest, respectively. (*D*) Neural source of differential HEP localized in the bilateral ACC extending to superior medial frontal gyrus (peak MNI coordinate: [14 40 20]; cluster size: 179 vertices). E–G: Effects of network connectivity in the gamma band (30–48 Hz). (*E*) Significant differential network topographies in the gamma band with each link indicating a connection. (*F*) Top 4 most connected regions within the significant network in *E*. Each node represents a brain region with its size indicating the number of connections within the network (degree). IFGopere.L: left inferior frontal gyrus, opercular part; SFGdor.R: right superior frontal gyrus, dorsolateral part; CAU.L: left caudate nucleus; INS.L: left insula. (*G*) Mean gamma connectivity strength within the identified network in *E* of monk meditation and rest conditions. (*H*) Significant correlation between HEP differential modulation and gamma network connectivity modulation ($r = 0.44$, $P < 1 \times 10^{-3}$).

middle temporal pole, right superior temporal pole, left inferior frontal gyrus, opercular part, and right gyrus rectus (Fig. 4B; 31 regions, 78 connections; Supplementary Table S4).

Strong Unique Gamma to Theta Directional Coupling during Monk Meditation

Driven by the well-established assumption that neuronal oscillations are interactive rather than functionally independent (Jensen and Colgin 2007; Canolty and Knight 2010), we further investigated the CFD of our EEG recordings. In this technique, estimates of the directional influence of one frequency's phase on another's power are determined and are typically calculated by separating the spectrum into either high or low frequencies (Jiang et al. 2015). It is hypothesized that a positive CFD value indicates that the phase of the slow oscillations informs and directs the high-frequency power and that a negative value indicates the converse. Here, the CFD values were calculated for the entire brain, using the phase and amplitude estimates of the 2–22 Hz and 30–120 Hz ranges, respectively, and were subsequently averaged over subjects for all paired ROIs within all conditions (control rest, monk rest, and monk mediation; Fig. 5). Interestingly, we observed a strong, unique negative CFD between theta (4–8 Hz) phase and gamma (40–80 Hz) amplitude during the Buddhist monks' meditation (Fig. 5A), indicating that the power of gamma oscillations resets the phase of theta oscillations during meditation. After averaging the CFD in the theta and gamma frequency ranges, we found that the gamma to theta CFD was significantly different between monk meditation and monk rest [$t(102) = -1.9$, $P < 0.05$] but not between monk rest and control rest [$t(75) = -0.84$, $P > 0.50$; Fig. 5B].

Discussion

In this work, we have investigated the neurovisceral coupling and spontaneous large-scale spatiotemporal brain network activity underlying meditation in a unique and rare data set. Specifically, we have demonstrated that the immediate effects of meditation in skilled meditation practitioners include transient changes in the neural activity of the ACC in response to heartbeats and decreased frontal-limbic network connectivity in the gamma band. Additionally, long-term meditation produced persistent effects, primarily altering the cortical relationship with cardiac signals in the PCC/precuneus/right mPFC and attenuating parietal-central and parietal-limbic network connectivity in the theta band. We further demonstrated that the monk resting-state temporal-frontal network connectivity in the theta band negatively correlated with meditation experience and that gamma oscillations were uniquely, directionally coupled to theta oscillations during the monks' meditation. Taken together, the present findings provide evidence for meditation's ability to induce the reorganization of cardiac influenced neuronal activity and the underlying spatiotemporal brain networks.

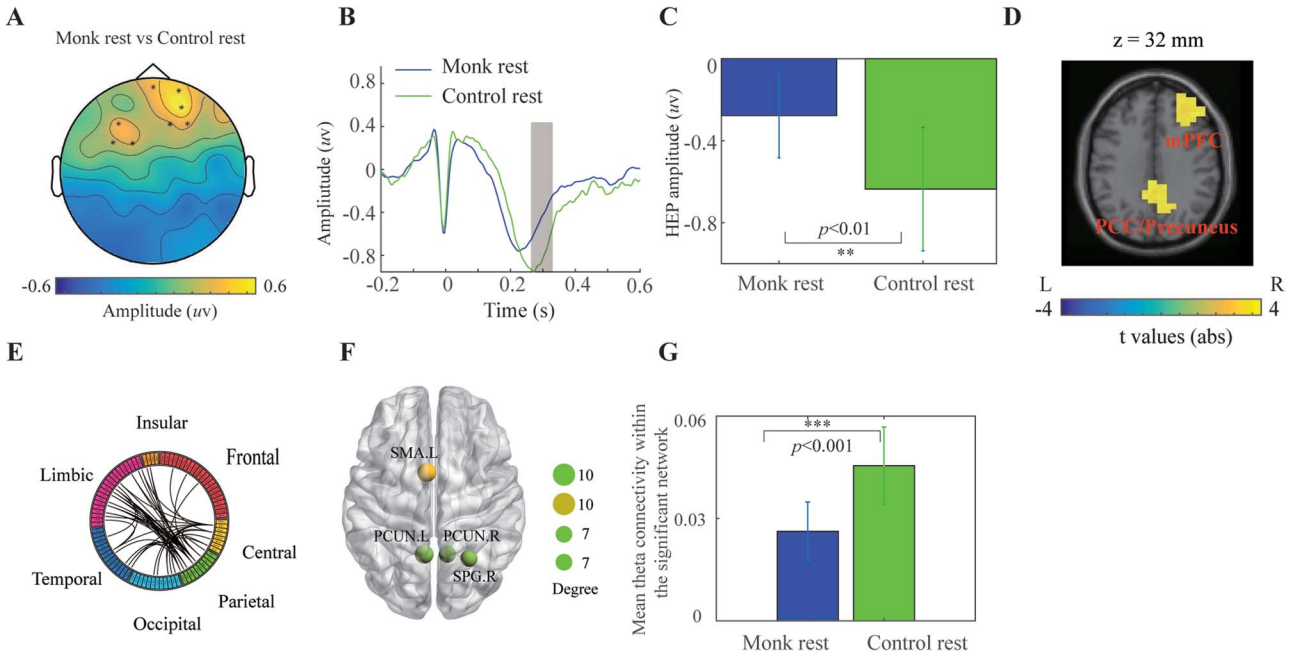

Figure 3. Long-term meditation effects determined by comparing monk rest to control rest. A–D: HEP effects. (A) HEP topological difference maps during the 280–320 ms following the R peak in which a significant difference is observed. Dots mark the locations of sensors above significant clusters. (B) Time course of the HEP averaged across the marked sensors in A. The shaded region indicates the time period in which significant differences are identified through cluster statistics (cluster level, $P < 0.05$). (C) Mean HEP amplitude averaged across the marked sensors during the 280–320 ms following the R peak for monk rest and control rest, respectively. (D) The neural sources of the differential HEP were localized to 2 clusters containing multiple regions: one extending across the PCC and precuneus bilaterally (peak MNI coordinates: [−1 −37 32]; cluster size: 147 vertices) and the other in the right mPFC (peak MNI coordinates: [34 32 34]; cluster size: 81 vertices). E–G: Effects of network connectivity in the theta band (4–8 Hz). (E) Significantly different network topographies in the theta band. (F) Top 4 most connected regions within the significant network in E. Each node represents a brain region with the size indicating the number of connections within the network (degree). PCUN.R: right precuneus; PCUN.L: left precuneus; SPG.R: right superior parietal gyrus; SMA.L: left supplementary motor area. (G) Mean theta connectivity strengths of monk rest and control rest conditions within the identified network in E.

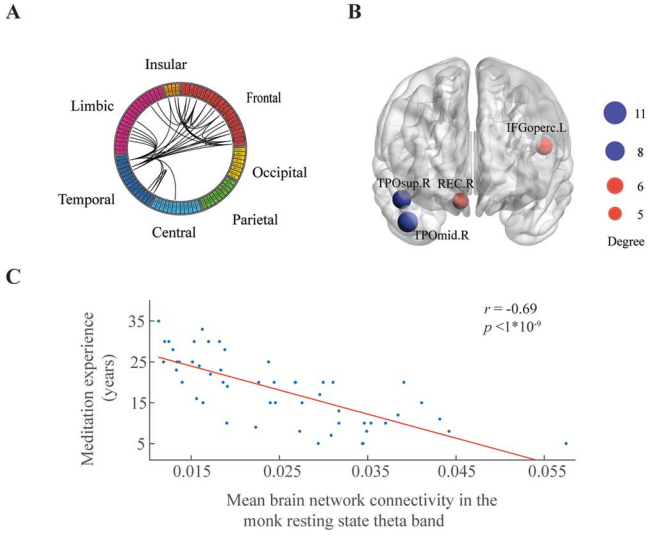

Figure 4. Correlation between the brain network connectivity in the monk resting-state theta band (4–8 Hz) and meditation experience. (A) Significant network topographies in the theta band correlated with meditation experience. (B) Top 4 most connected regions within the significant network in A. Each node represents a single brain region with the size indicating the number of connections within the network (degree). TPOmid.R: right middle temporal pole; TPOsup.R: right superior temporal pole; IFGoperc.L: left inferior frontal gyrus, opercular part; REC.R: right gyrus rectus. (C) Correlation between mean network connectivity (in A) in the monk resting-state theta band and meditation experience ($r = -0.69$, $P < 1 \times 10^{-9}$).

Our HEP results are consistent with previous investigations concerning the neural response to heartbeats, in that the effects were typically found to exist between 200 ms and 500 ms after ECG R peaks (Montoya et al. 1993; Pollatos and Schandry 2004). Here, the immediate and persistent effects of meditation on HEPs specifically occurred in the 340 ms–360 ms and

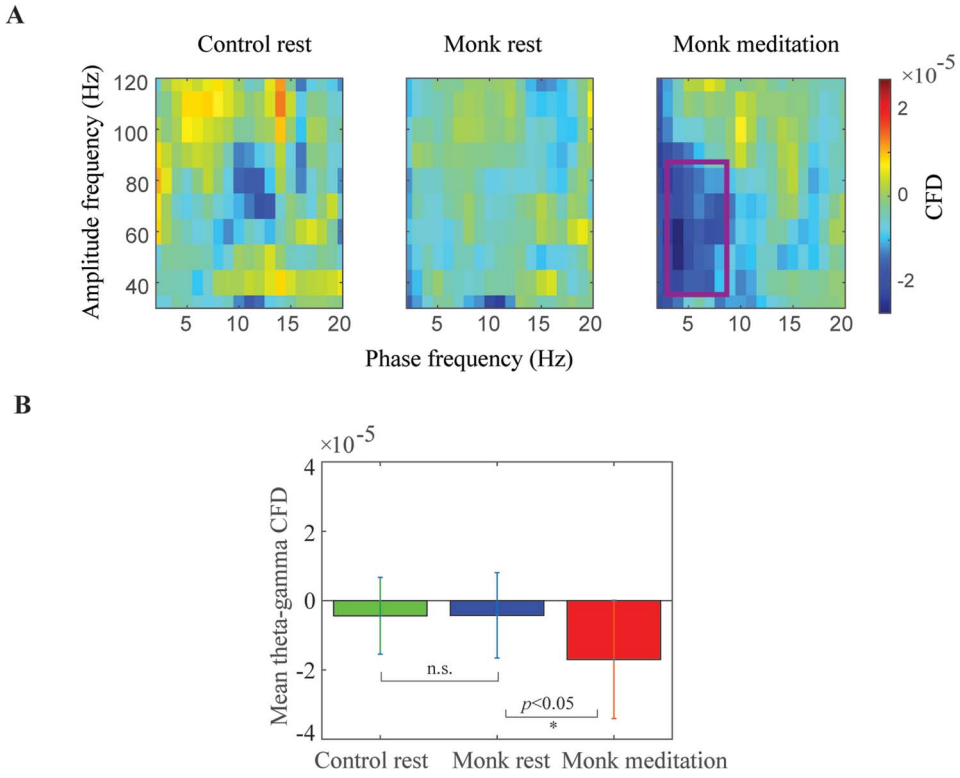

Figure 5. CFD during control rest, monk rest, and monk meditation conditions. (A) CFD averaged over all paired ROIs across subjects and conditions. CFD was computed in the phase frequencies ranging from 2 to 22 Hz and amplitude frequencies from 30 to 120 Hz. (B) Mean CFD between 4–8 Hz theta phase frequency and 40-80 Hz gamma amplitude frequency. Error bars represent standard deviations across subjects. Significant differences were found between monk meditation and monk rest conditions [$t(102) = -1.9$, $P < 0.05$] but not between monk rest and control rest conditions [$t(75) = -0.84$, $P > 0.50$].

280 ms–320 ms time-periods following the R peak, respectively. Our work further corroborates the findings expressed in literature that the neural pathways between cardiac activity and the neocortex primarily involve the somatosensory cortex, mPFC, cingulate cortex, insula, and amygdala (Park et al. 2014; Park et al. 2016; Park et al. 2018). In particular, the HEP differential sources discerned here mainly lie in the bilateral ACC, bilateral PCC, and right mPFC, all typical heartbeat-related processing regions. Additionally, we conducted surrogate R peak control analyses to exclude the possibility that the observed HEP effects were due to random EEG activity fluctuations.

It has been hypothesized that the HEP represents the cortical processing of cardiac information and creates the neural subjective frame that is critical for subjective experiences, self-conscious, and emotional feelings (Park and Tallon-Baudry 2014). Further studies have shown that the HEP was directly linked to visual conscious perception detection (Park et al. 2014), state of bodily self-consciousness (Park et al. 2016), and self-related processing (Babo-Rebelo et al. 2016). Unlike other forms of meditation, Tibetan Buddhist meditation typically involves focusing on reciting a mantra or imagining a Buddha. In this form of focused attention meditation, an individual's perception of their cardiac activity is not the object of meditation, but rather serves as a potential distractor, briefly catching the monks' attention before being disregarded. Therefore, we infer that the monks were not constantly aware of their cardiac activity during meditation and that the change in HEP observed here occurs at the subconscious level. During meditation, compared to rest, the HEP was found to significantly differ in the ACC, a region well known for conflict monitoring (van Veen et al. 2001). While the observed change in HEP amplitude could be due to heart rate, heart rate variability, and ECG amplitude changes, these basic cardiorespiratory measures did not differ between conditions (Supplementary Fig. S2). Moreover, the data cleaning and HEP processing procedure removed equivalent artifacts from all conditions (Supplementary Fig. S3). Thus, it is highly likely that the HEP change observed here reflects true changes in brain activities locked to the heartbeat, rather than other potential confounds, and that the decrease in ACC HEP amplitude reflects a reduction in internal conflict, either consciously or subconsciously. More specifically, we interpret this reduction in ACC HEP amplitude to mean that during meditation the Tibetan Buddhist monks focus solely on their meditative strategy and remain completely ambivalent to any potential distractors, especially, internally generated cardiac activity.

Outside of investigating the direct interactions between the HEP and meditative practices, we further considered the influences meditation may have on the spatiotemporal network level dynamics. The changes in the temporal aspects of neural integration during and in response to meditation span across different frequencies, many of which are associated with different functional and behavioral demands (Buzsaki and Draguhn 2004), and whose interactions can be determined through cross-frequency coupling (CFC) (Jensen and Colgin 2007; Canolty and Knight 2010). The alterations in the spatial aspects of integration involve the in/exclusion of nodes and specific properties of the networks involved. In concert with the findings of previous studies, which have examined experienced meditators and

have described elevated gamma activities and their potential involvement in "internally generated stimuli" processing (Lutz et al. 2004), we found increased posterior gamma activities and decreased frontal-limbic network connectivity in the gamma band during meditation. Synchronized gamma serves as a gain control for mental processing (Salinas and Sejnowski 2001) and enables postsynaptic potentials to integrate, directing downstream networks to bind the elements of sensory processing to a perceptual object (von Stein and Sarnthein 2000). It has been shown that gamma activity is higher when actively maintaining abstract visual shapes in short-term memory and when subjects attend to stimuli, compared to unattended stimuli (Jensen et al. 2007). In line with the concept of internally generated stimuli, we speculate that these enhanced posterior gamma activities during meditation reflect the processing of either the "visual Buddha imaginary" or the "visual representation of the mantra". Additionally, hyper connectivity in gamma band has been suggested to be a signature of loss of consciousness, which is common across different anesthetic agent manipulations in different wake–sleep stages (Bola et al. 2018). Therefore, the attuned frontal-limbic network connectivity in the gamma band potentially indicates the meta-awareness/consciousness state hypothesized to be involved in meditation. Moreover, monks exhibited unique, strong gamma to theta directional coupling during meditation, which, based on the significant evidence implicating theta–gamma coupling's importance in attentional tasks (Canolty et al. 2006; Voloh et al. 2015), we believe to be directly related to the monks' attentional focus and processing. Research has also shown that couplings between slow and fast frequencies correspond to different levels or consciousness (Northoff and Huang 2017). For instance, the misbalance of slow and fast frequencies, e.g., weaker gamma activity (20–60 Hz) and stronger delta activity (1–4 Hz), was found in anesthesia and unresponsive wakefulness states (Lewis et al. 2012; Purdon et al. 2013; Sitt et al. 2014). Notably, an EEG study showed that alpha amplitudes were maximal at low frequency peaks during profound unconsciousness, while the relationship was reversed during the transition into and out of unconsciousness (Purdon et al. 2013). Therefore, the observed gamma–theta directional coupling during meditation probably signifies the achievement of the hypothesized "unique state of consciousness" (Michaels et al. 1976) and involves large-scale hierarchical reorganizations of temporal activity.

Besides observing unique changes, which existed during meditation, several studies have previously reported meditation induced long-term changes in brain structure (Lazar et al. 2005), attentional processing (Carter et al. 2005), and emotional processing (Goldin and Gross 2010). In line with those studies, we too found network level persistent changes, including decreased frontal theta activity and attenuated parietal-central and parietal-limbic network connectivity in the theta band in long-term meditators. Frontal theta activity has been suggested to be a candidate biophysical mechanism for cognitive control (Cavanagh and Frank 2014). In simultaneous EEG/fMRI studies, frontal theta activity is often inversely correlated with activity in DMN (Scheeringa et al. 2008; Murta et al. 2015), a brain network implicated in self-related thinking and mind wandering (Mason et al. 2007; Brewer et al. 2011). Therefore, the lower trait theta power and connectivity in Tibetan monk meditators might indicate an ability to limit the processing of unnecessary information (e.g., discursive thought) and a reduction in mind wandering (Tanaka et al. 2014). HEP cortical representations were also altered in the PCC/precuneus/right mPFC, all key DMN regions, during the monk resting-state recordings. Besides being highly active during wakeful rest, the DMN also plays an important role in central autonomic function (Thayer et al. 2012; Beissner et al. 2013). Overall, these results suggest that meditation changes the "baseline" activity of the brain, potentially influencing spontaneous self-regulatory processes and cardiac monitoring, primarily through the DMN. Notably, the monk resting-state temporal-frontal network connectivity in the theta band negatively correlated with meditation experience, suggesting that meditation training may constantly take advantage of cortical plasticity and induce gradual changes. Future studies will need to examine how and to what extent meditation practice can affect cognitive function and behavior in daily life.

With both HEP and spatiotemporal network level modifications identified, we further hypothesized that their coexistence during meditation was noncoincidental and that a specific functional connection between the 2 could be discerned. In our investigation, we found that during meditation the ACC-localized HEP and the modulation of frontal-limbic network connectivity in the gamma band were highly correlated. Notably, the analysis of time-frequency representations also showed increased gamma activity during the window previously identified to contain significant differences in HEP modulation during meditation (Supplementary Fig. S4), providing further electrophysiological evidence for the observed correlation between HEP modulation and gamma activity/connectivity. This concept that the integration of temporal interactions between the heartbeat and the intrinsic spatiotemporal neural activity is fundamental to meditation is further supported by numerous studies. Of these studies, some more prominent works have demonstrated tight functional coupling between self-related processing and cardiac monitoring in the DMN (Babo-Rebelo et al. 2016), correlated frontal midline ACC theta activity with high-frequency heart rate variability after 5 days of integrative body–mind training (Tang et al. 2009), and stronger positive coupling in the dorsal ACC between heart rate and BOLD within the compassion meditation states compared to the neutral state (Lutz et al. 2009). These brain–heart interactions and network dynamics provide an integrative neural framework, which appears to be critical for meditation. However, further interpretations from our findings should be made cautiously. The brain–heart couplings underlying meditation found in this work were essentially correlative and therefore cannot reveal any causal relationships between HEP modulations and spontaneous brain network alterations.

Although our findings are significant and suggest underlying mechanisms for alterations from meditation, a few limitations exist within the presented study and data set. Primarily, we and the field as a whole have no objective method for determining if subjects were "properly" meditating. Additionally, we did not attempt to estimate this, as the inclusion of behavioral measures or tasks potentially disrupts ongoing meditation. Furthermore, it has been suggested that long-term meditators can reproducibly generate stable mental states, when compared with naïve subjects (Lutz et al. 2007), diminishing the possibility of "unsuccessful meditation". In this work, all meditators were long-term Tibetan Buddhist monks with at least 5 years of meditation experience who reported that their meditative experience during the experiment was equivalent to their daily mediation practice. However, even with this robust and unique data set, it is quite challenging to identify the precise cognitive components underlying meditation. Lastly, other than heartbeats, visceral activity, such as one's gastric basal rhythm, might be relevant

during meditation. Significant CFC between the infraslow gastric phase (~0.05 Hz) and the amplitude of the cortical alpha rhythm (10–11 Hz) has previously been demonstrated during resting-state conditions, with gastric phase accounting for 8% of the variance of fluctuations in the alpha rhythm amplitude (Richter et al. 2017). Given the importance of mind–body interactions in meditation discerned here, it might be interesting and necessary to investigate the potentially altered brain–stomach interactions underlying meditation as well.

In conclusion, we discovered a relationship between the neural response to heartbeats in the DMN and the reorganization of large-scale network dynamics at different frequencies in response to meditation. Our findings provide direct neural evidence for the hypothesized link between the brain's ability to process cardiac activity and meditation. Overall, these results suggest that not only independent CNS processing, but also the neural response to cardiac rhythms, contribute to the fundamental neural mechanism of meditation. Thus, future work should focus on the mind–body interactions of mediation through the joint investigation of physiological and brain signals.

Funding

Chinese "111 Project" (B08020); Medtronic-Bakken Endowed Chair; Natural Science Foundation of Shanghai (17ZR1445300); and Shanghai Jiao Tong University Grants (YG2016ZD06 and 14JCRZ05).

Notes

We would like to thank Prof. Lisa Xu for her encouragement and support of this international collaboration, Kambo Suo Lang and Kambo Kharong for their help in recruiting monks and local control subjects, and Dr Brad Edelman for his comments on the manuscript. We would also like to thank the monks from Qiongke Temple and Jiaqu temple and the local control subjects for their participation.

References

Babo-Rebelo M, Richter CG, Tallon-Baudry C. 2016. Neural responses to heartbeats in the default network encode the self in spontaneous thoughts. *J Neurosci*. 36:7829–7840.

Beissner F, Meissner K, Bar KJ, Napadow V. 2013. The autonomic brain: an activation likelihood estimation meta-analysis for central processing of autonomic function. *J Neurosci*. 33:10503–10511.

Bola M, Barrett AB, Pigorini A, Nobili L, Seth AK, Marchewka A. 2018. Loss of consciousness is related to hyper-correlated gamma-band activity in anesthetized macaques and sleeping humans. *NeuroImage*. 167:130–142.

Brewer JA, Worhunsky PD, Gray JR, Tang YY, Weber J, Kober H. 2011. Meditation experience is associated with differences in default mode network activity and connectivity. *Proc Natl Acad Sci U S A*. 108:20254–20259.

Buzsaki G, Draguhn A. 2004. Neuronal oscillations in cortical networks. *Science*. 304:1926–1929.

Canolty RT, Edwards E, Dalal SS, Soltani M, Nagarajan SS, Kirsch HE, Berger MS, Barbaro NM, Knight RT. 2006. High gamma power is phase-locked to theta oscillations in human neocortex. *Science*. 313:1626–1628.

Canolty RT, Knight RT. 2010. The functional role of cross-frequency coupling. *Trends Cogn Sci*. 14:506–515.

Carter OL, Presti DE, Callistemon C, Ungerer Y, Liu GB, Pettigrew JD. 2005. Meditation alters perceptual rivalry in Tibetan Buddhist monks. *Curr Biol*. 15:R412–R413.

Cavanagh JF, Frank MJ. 2014. Frontal theta as a mechanism for cognitive control. *Trends Cogn Sci*. 18:414–421.

Craig AD. 2009. How do you feel—now? The anterior insula and human awareness. *Nature Rev Neurosci*. 10:59.

Davidson RJ, Lutz A. 2008. Buddha's brain: neuroplasticity and meditation. *IEEE Signal Process Mag*. 25:176–174.

Ekman P, Davidson RJ, Ricard M, Wallace BA. 2005. Buddhist and psychological perspectives on emotions and well-being. *Curr Dir Psychol Sci*. 14:59–63.

Goldin PR, Gross JJ. 2010. Effects of mindfulness-based stress reduction (MBSR) on emotion regulation in social anxiety disorder. *Emotion*. 10:83–91.

Gross J, Kujala J, Hamalainen M, Timmermann L, Schnitzler A, Salmelin R. 2001. Dynamic imaging of coherent sources: studying neural interactions in the human brain. *Proc Natl Acad Sci U S A*. 98:694–699.

Gu Z, Gu L, Eils R, Schlesner M, Brors B. 2014. circlize implements and enhances circular visualization in R. *Bioinformatics*. 30:2811–2812.

He B, Yang L, Wilke C, Yuan H. 2011. Electrophysiological imaging of brain activity and connectivity-challenges and opportunities. *IEEE Trans Biomed Eng*. 58:1918–1931.

Holzel BK, Lazar SW, Gard T, Schuman-Olivier Z, Vago DR, Ott U. 2011. How does mindfulness meditation work? Proposing mechanisms of action from a conceptual and neural perspective. *Perspect Psychol Sci*. 6:537–559.

Jensen O, Colgin LL. 2007. Cross-frequency coupling between neuronal oscillations. *Trends Cogn Sci*. 11:267–269.

Jensen O, Kaiser J, Lachaux JP. 2007. Human gamma-frequency oscillations associated with attention and memory. *Trends Neurosci*. 30:317–324.

Jiang H, Bahramisharif A, van Gerven MA, Jensen O. 2015. Measuring directionality between neuronal oscillations of different frequencies. *NeuroImage*. 118:359–367.

Johnson C. 2004. *Essentials of Mahamudra: looking directly at the mind*. Somerville, MA: Wisdom Publications.

Lazar SW, Kerr CE, Wasserman RH, Gray JR, Greve DN, Treadway MT, McGarvey M, Quinn BT, Dusek JA, Benson H *et al*. 2005. Meditation experience is associated with increased cortical thickness. *Neuroreport*. 16:1893–1897.

Levine GN, Lange RA, Bairey-Merz CN, Davidson RJ, Jamerson K, Mehta PK, Michos ED, Norris K, Ray IB, Saban KL *et al*. 2017. Meditation and cardiovascular risk reduction: a scientific statement from the American Heart Association. *J Am Heart Assoc*. 6:1–14.

Lewis LD, Weiner VS, Mukamel EA, Donoghue JA, Eskandar EN, Madsen JR, Anderson WS, Hochberg LR, Cash SS, Brown EN *et al*. 2012. Rapid fragmentation of neuronal networks at the onset of propofol-induced unconsciousness. *Proc Natl Acad Sci U S A*. 109:E3377–E3386.

Lutz A, Dunne JD, Davidson RJ. 2007. Meditation and the neuroscience of consciousness: an introduction. In: Thompson E, Moscovitch M, Zelazo PD, editors. *The Cambridge handbook of consciousness*. Cambridge: Cambridge University Press

Lutz A, Greischar LL, Perlman DM, Davidson RJ. 2009. BOLD signal in insula is differentially related to cardiac function during compassion meditation in experts vs. novices. *NeuroImage*. 47:1038–1046.

Lutz A, Greischar LL, Rawlings NB, Ricard M, Davidson RJ. 2004. Long-term meditators self-induce high-amplitude gamma synchrony during mental practice. *Proc Natl Acad Sci U S A*. 101:16369–16373.

Maris E, Oostenveld R. 2007. Nonparametric statistical testing of EEG- and MEG-data. *J Neurosci Methods*. 164:177–190.

Mason MF, Norton MI, Van Horn JD, Wegner DM, Grafton ST, Macrae CN. 2007. Wandering minds: the default network and stimulus-independent thought. *Science*. 315:393–395.

Michaels R, Huber M, McCann D. 1976. Evaluation of transcendental meditation as a method of reducing stress. *Science*. 192:1242–1244.

Montoya P, Schandry R, Muller A. 1993. Heartbeat evoked potentials (HEP): topography and influence of cardiac awareness and focus of attention. *Electroencephalogr Clin Neurophysiol*. 88:163–172.

Murta T, Leite M, Carmichael DW, Figueiredo P, Lemieux L. 2015. Electrophysiological correlates of the BOLD signal for EEG-informed fMRI. *Hum Brain Mapp*. 36:391–414.

Muthukumaraswamy SD. 2013. High-frequency brain activity and muscle artifacts in MEG/EEG: a review and recommendations. *Front Hum Neurosci*. 7:138.

Nolte G, Bai O, Wheaton L, Mari Z, Vorbach S, Hallett M. 2004. Identifying true brain interaction from EEG data using the imaginary part of coherency. *Clin Neurophysiol*. 115: 2292–2307.

Nolte G, Ziehe A, Nikulin VV, Schlogl A, Kramer N, Brismar T, Muller KR. 2008. Robustly estimating the flow direction of information in complex physical systems. *Phys Rev Lett*. 100:234101.

Northoff G, Huang Z. 2017. How do the brain's time and space mediate consciousness and its different dimensions? Temporo-spatial theory of consciousness (TTC). *Neurosci Biobehav Rev*. 80:630–645.

Oostenveld R, Fries P, Maris E, Schoffelen JM. 2011. FieldTrip: open source software for advanced analysis of MEG, EEG, and invasive electrophysiological data. *Comput Intell Neurosci*. 2011:156869.

Park HD, Bernasconi F, Bello-Ruiz J, Pfeiffer C, Salomon R, Blanke O. 2016. Transient modulations of neural responses to heartbeats covary with bodily self-consciousness. *J Neurosci*. 36:8453–8460.

Park HD, Bernasconi F, Salomon R, Tallon-Baudry C, Spinelli L, Seeck M, Schaller K, Blanke O. 2018. Neural sources and underlying mechanisms of neural responses to heartbeats, and their role in bodily self-consciousness: an intracranial EEG study. *Cereb Cortex*. 28:2351–2364.

Park HD, Correia S, Ducorps A, Tallon-Baudry C. 2014. Spontaneous fluctuations in neural responses to heartbeats predict visual detection. *Nat Neurosci*. 17:612–618.

Park HD, Tallon-Baudry C. 2014. The neural subjective frame: from bodily signals to perceptual consciousness. *Philos Trans R Soc Lond B Biol Sci*. 369:20130208.

Pollatos O, Schandry R. 2004. Accuracy of heartbeat perception is reflected in the amplitude of the heartbeat-evoked brain potential. *Psychophysiology*. 41:476–482.

Purdon PL, Pierce ET, Mukamel EA, Prerau MJ, Walsh JL, Wong KF, Salazar-Gomez AF, Harrell PG, Sampson AL, Cimenser A *et al*. 2013. Electroencephalogram signatures of loss and recovery of consciousness from propofol. *Proc Natl Acad Sci U S A*. 110:E1142–E1151.

Razumnikova OM. 2007. Creativity related cortex activity in the remote associates task. *Brain Res Bull*. 73:96–102.

Richter CG, Babo-Rebelo M, Schwartz D, Tallon-Baudry C. 2017. Phase-amplitude coupling at the organism level: the amplitude of spontaneous alpha rhythm fluctuations varies with the phase of the infra-slow gastric basal rhythm. *NeuroImage*. 146:951–958.

Rubia K. 2009. The neurobiology of meditation and its clinical effectiveness in psychiatric disorders. *Biol Psychol*. 82:1–11.

Saggar M, King BG, Zanesco AP, Maclean KA, Aichele SR, Jacobs TL, Bridwell DA, Shaver PR, Rosenberg EL, Sahdra BK *et al*. 2012. Intensive training induces longitudinal changes in meditation state-related EEG oscillatory activity. *Front Hum Neurosci*. 6:256.

Salinas E, Sejnowski TJ. 2001. Correlated neuronal activity and the flow of neural information. *Nat Rev Neurosci*. 2:539–550.

Scheeringa R, Bastiaansen MC, Petersson KM, Oostenveld R, Norris DG, Hagoort P. 2008. Frontal theta EEG activity correlates negatively with the default mode network in resting state. *Int J Psychophysiol*. 67:242–251.

Sitt JD, King JR, El Karoui I, Rohaut B, Faugeras F, Gramfort A, Cohen L, Sigman M, Dehaene S, Naccache L. 2014. Large scale screening of neural signatures of consciousness in patients in a vegetative or minimally conscious state. *Brain*. 137:2258–2270.

Tanaka GK, Peressutti C, Teixeira S, Cagy M, Piedade R, Nardi AE, Ribeiro P, Velasques B. 2014. Lower trait frontal theta activity in mindfulness meditators. *Arq Neuropsiquiatr*. 72:687–693.

Tang YY, Holzel BK, Posner MI. 2015. The neuroscience of mindfulness meditation. *Nat Rev Neurosci*. 16:213–225.

Tang YY, Ma Y, Fan Y, Feng H, Wang J, Feng S, Lu Q, Hu B, Lin Y, Li J *et al*. 2009. Central and autonomic nervous system interaction is altered by short-term meditation. *Proc Natl Acad Sci U S A*. 106:8865–8870.

Thayer JF, Ahs F, Fredrikson M, Sollers JJ 3rd, Wager TD. 2012. A meta-analysis of heart rate variability and neuroimaging studies: implications for heart rate variability as a marker of stress and health. *Neurosci Biobehav Rev*. 36:747–756.

Thayer JF, Lane RD. 2000. A model of neurovisceral integration in emotion regulation and dysregulation. *J Affect Disord*. 61:201–216.

Tzourio-Mazoyer N, Landeau B, Papathanassiou D, Crivello F, Etard O, Delcroix N, Mazoyer B, Joliot M. 2002. Automated anatomical labeling of activations in SPM using a macroscopic anatomical parcellation of the MNI MRI single-subject brain. *NeuroImage*. 15:273–289.

Van Veen BD, van Drongelen W, Yuchtman M, Suzuki A. 1997. Localization of brain electrical activity via linearly constrained minimum variance spatial filtering. *IEEE Trans Biomed Eng*. 44:867–880.

van Veen V, Cohen JD, Botvinick MM, Stenger VA, Carter CS. 2001. Anterior cingulate cortex, conflict monitoring, and levels of processing. *NeuroImage*. 14:1302–1308.

Voloh B, Valiante TA, Everling S, Womelsdorf T. 2015. Theta-gamma coordination between anterior cingulate and prefrontal cortex indexes correct attention shifts. *Proc Natl Acad Sci U S A*. 112:8457–8462.

von Stein A, Sarnthein J. 2000. Different frequencies for different scales of cortical integration: from local gamma to long range alpha/theta synchronization. *Int J Psychophysiol*. 38:301–313.

Wallace BA. 2006. *The attention revolution : unlocking the power of the focused mind*. Boston: Wisdom Publications

Wallace RK. 1970. Physiological effects of transcendental meditation. *Science*. 167:1751–1754.

Wong SW, Masse N, Kimmerly DS, Menon RS, Shoemaker JK. 2007. Ventral medial prefrontal cortex and cardiovagal control in conscious humans. *NeuroImage*. 35:698–708.

Xia M, Wang J, He Y. 2013. BrainNet Viewer: a network visualization tool for human brain connectomics. *PLoS One*. 8:e68910.

Zalesky A, Fornito A, Bullmore ET. 2010. Network-based statistic: identifying differences in brain networks. *NeuroImage*. 53:1197–1207.

Ziegler G, Dahnke R, Yeragani VK, Bar KJ. 2009. The relation of ventromedial prefrontal cortex activity and heart rate fluctuations at rest. *Eur J Neurosci*. 30:2205–2210.